



## Original Articles

# Cullin7 enhances resistance to trastuzumab therapy in Her2 positive breast cancer via degrading IRS-1 and downregulating IGFBP-3 to activate the PI3K/AKT pathway

Ni Qiu<sup>a,1</sup>, Yu-fang He<sup>a,1</sup>, Si-ming Zhang<sup>b</sup>, Yong-tao Zhan<sup>a</sup>, Guo-dong Han<sup>a</sup>, Ming Jiang<sup>a</sup>, Wei-xing He<sup>a</sup>, Jie Zhou<sup>a</sup>, Hong-ling Liang<sup>a</sup>, Xiang Ao<sup>a</sup>, Hao-ming Xia<sup>a</sup>, Jia Li<sup>c</sup>, Yu-yang Yang<sup>b</sup>, Zhi-min He<sup>a</sup>, Zheng-zhi Zou<sup>d,\*\*</sup>, Hong-sheng Li<sup>a,\*</sup>

<sup>a</sup> Department of Breast Surgery, Affiliated Cancer Hospital & Institute of Guangzhou Medical University, Guangzhou, 510095, PR China

<sup>b</sup> Department of Breast Surgery, Meizhou People's Hospital, Meizhou, 514000, PR China

<sup>c</sup> South China University of Technology, Guangzhou, 510641, PR China

<sup>d</sup> MOE Key Laboratory of Laser Life Science & Institute of Laser Life Science, College of Biophotonics, South China Normal University, Guangzhou, 510631, PR China

## ARTICLE INFO

## Keywords:

Drug resistance  
Cullin7  
Her2-amplified breast cancer  
Insulin receptor Substrate-1

## ABSTRACT

Patients with Her2-positive breast cancer exhibit *de novo* resistance or develop acquired resistance in less than one year after Her2 targeting treatment, but the mechanism is not fully elucidated. Compensatory pathways such as the IGF-1R/IRS-1 pathway, are activated, leading to aberrant enhanced PI3K/Akt/mTOR pathway activity to attenuate the efficacy of trastuzumab. Cullin7 could participate in the degradation of IRS-1 in a mTOR/S6K dependent manner. Whether Cullin7 participates in trastuzumab resistance needs to be further investigated. Here, we reveals that Cullin7 is overexpressed in trastuzumab-resistant Her2 positive breast cancer cells. Knockdown of Cullin7 reduces degradation of Ser phosphorylation of IRS-1, attenuates activation of the PI3K/AKT pathway, and partly restores trastuzumab sensitivity in trastuzumab-resistant Her2 positive breast cancer cells. IGFBP-3 expression is decreased in trastuzumab-resistant Her2 positive breast cancer cells, which leads to release of the Wnt signaling pathway inhibition and an increase in Cullin7 expression, as mediated by TCF7L2. Overexpression of Cullin7 in Her2-amplified breast cancer tissues has clinical implications because it positively correlates with shorter disease-free survival (DFS) and inadequate response to trastuzumab. Thus, our results suggest a critical role for Cullin7 in response to trastuzumab, which has significant implications for selection of the optimal therapeutic strategy for Her2 positive breast cancers.

## 1. Introduction

Breast cancer heterogeneity is closely associated with response rates, disease progression and overall survival [1–3]. Her2 positive breast cancer, a breast cancer subtype with overexpression or amplification of the Her2 oncogene, has an aggressive clinical course and a worse prognosis [4–6]. Her2-targeting agents such as trastuzumab, lapatinib, pertuzumab and trastuzumab-DM1 (T-DM1) significantly improve patient survival [7–9]. However, approximately 50% of Her2-amplified patients exhibit *de novo* resistance or develop acquired resistance in less than one year [10–14]. Thus, the resistance to these

Her2 targeting agents has become a considerable obstacle to the treatment of Her2-positive breast cancer patients.

Her2 is a member of the ErbB family of receptor tyrosine kinases. Her2 mediates signal transduction through heterodimerization with other ErbB family members, including Erb1, Erb3, and Erb4 [15]. Heterodimerization causes autophosphorylation of the tyrosine kinase domain of the receptor and subsequent activation of downstream pathways, including the phosphoinositide 3-kinase/protein kinase B/mammalian target of rapamycin (PI3K/Akt/mTOR) and Ras/Raf/mitogen-activated protein kinase (MAPK) pathways [4,16–18]. IGF-1R phosphorylates the insulin receptor substrate-1 (IRS-1) at the tyrosine

\* Corresponding author. Department of Breast Surgery, Affiliated Cancer Hospital & Institute of Guangzhou Medical University, No. 78 Hengzhigang Road, Guangzhou, 510095, PR China.

\*\* Corresponding author.

E-mail addresses: [zouzhengzhi@m.scnu.edu.cn](mailto:zouzhengzhi@m.scnu.edu.cn) (Z.-z. Zou), [lihongsheng@gzhmu.edu.cn](mailto:lihongsheng@gzhmu.edu.cn) (H.-s. Li).

<sup>1</sup> Co-first authors.

site, leading to aberrant activation of downstream signaling pathways, such as the PI3K/Akt pathway [19–21].

IRS-1 belongs to the IRS family of adaptor molecules, and it is activated and phosphorylated on a tyrosine residue in response to insulin, insulin-like growth factor-1 and cytokines; further, it plays a vital role in organismal growth and tumorigenesis [22–24]. Deregulation of IRS-1 has been implicated in the pathogenesis of type II diabetes and cancer [23,25]. High IRS-1 expression levels are considered to be associated with worse outcomes and lymphnode metastases in patients with breast cancer [26,27]. IRS-1 contains several potential tyrosine phosphorylation sites and 50 potential serine/threonine phosphorylation sites [28]. Tyrosine phosphorylated of IRS1 can recruit SH2 containing signal transducers including PI3K [26]. However, serine phosphorylation of IRS1 at critical sites can block tyrosine phosphorylation and prevent IRS-1 binding to the IR [29,30], acting as negative feedback for IRS-1 function and ultimately promoting IRS-1 degradation and insulin resistance [28]. The chemotherapy drug Taxol induces the phosphorylation of IRS-1 at serine sites to restrain the survival effect of IGF in human breast cancer cells [31]. Thus, a delicate balance of negative and positive signals via counteracting Ser and Tyr phosphorylation is the key step for IRS-1 function and downstream signaling activation. It is possible that the alteration of this equilibrium will result in pathological situations.

Cullin7 (Cul7) is a member of the cullin family that functions as scaffold proteins for E3 ubiquitin ligases by binding to substrate recognition subunit F-box protein Fbw8, Skp1, and the small RING finger protein ROC1 [32]. Deletion of Cul7 in mice leads to intrauterine growth retardation and perinatal death, strongly suggesting that the Cul7 E3 ligase has a pivotal role in intrauterine growth [33,34]. In addition, overexpression of Cul7 mRNA and protein was significantly associated with poor prognosis and metastasis in patients with non-small cell lung carcinoma and hepatocellular carcinoma, suggesting Cul7 as an oncogene [35,36]. Recent research revealed that Cul7 participated in the degradation of IRS-1 in a mTOR/S6K dependent manner. Elevated activation of the mTORC1/S6K pathway leads to hyperphosphorylation of IRS-1 at Ser residues, and Cul7 complexes specifically bind to hyperphosphorylated IRS-1 and degrade IRS-1 [37]. Whether Cul7-mediated degradation of IRS1 participates in trastuzumab resistance needs further elucidation.

In this study, we provide evidence that Cul7 is overexpressed in Her2 amplified trastuzumab-resistant breast cancer cells and tissues; Knockdown of Cul7 expression restores trastuzumab sensitivity. Cul7 acts as a mediator to degrade negative Ser-phosphorylated IRS-1, avoiding the accumulation of negative Ser-phosphorylated IRS-1 in the cytoplasm, and relieving the blocked tyrosine phosphorylation site of IRS-1 to transduce signaling to the downstream effectors PI3K and others, inducing resistance to the Her2 inhibitor. Our study thus supports the concept that Cullin7 is a predictive biomarker of response to trastuzumab in Her2-positive breast cancer patients.

## 2. Results

### 2.1. Trastuzumab resistance in Her2-amplified breast cancer cells was partly due to overexpression of Cullin7

RT-PCR and Western blot analysis revealed an increase in the expression of Cul7 mRNA and protein, respectively, in SKBR3-TR cells and BT474-TR cells compared to parental cells (Fig. 1A). To evaluate whether the overexpression of Cul7 was associated with trastuzumab resistance, we stably knocked down Cul7 in SKBR3-TR and BT474-TR cells by using Lenti-shRNA knockdown methods. RT-PCR and Western blot results showed that the respective mRNA and protein expression of Cul7 was significantly decreased more than 60% in SKBR3-TR shCul7-1 and BT-TR shCul7-1 cells compared with corresponding TR or TR-shCon cells (Fig. 1B and C).

Next, to confirm whether Cul7 expression is associated with

trastuzumab sensitivity, trastuzumab-resistant cells and Cul7-1 knockdown cells were treated with 2-fold serial dilutions of trastuzumab ranging from 12.5 to 100  $\mu\text{g/ml}$  for 6 days. As shown in Fig. 1D and E, knockdown of Cullin7 expression in TR cells increased trastuzumab sensitivity. Flow cytometry analysis also showed that in the presence of 20  $\mu\text{g/ml}$  trastuzumab for 72 h, the percentage of total cell apoptosis (including early and later apoptotic cells) was markedly increased to 47.3% and 30.8% in SKBR3-TR-shCul7 and BT474-TR-shCul7 cells, respectively, whereas trastuzumab had slight effects on the apoptosis of SKBR3-TR-shCon and BT474-TR-shCon cells, evidenced by the percentage of total apoptotic cells only 10.4% and 16%, respectively, in those cells (Fig. 1F). Those data indicated that the level of Cul7 expression is positively correlated with trastuzumab resistance.

Because trastuzumab mainly inhibits cell growth and induces cell senescence [38], we investigated the cell cycle in TR-shCon and TR-shCul7 cells after 20  $\mu\text{g/ml}$  trastuzumab treatment for 48 h by flow cytometry. We found that a greater percentage of cells was arrested in the G0/G1 stage in SKBR3-TR-shCul7 cells and BT474-TR-shCul7 cells treated with trastuzumab when compared with the corresponding TR-shCon, indicating that Cul7 knockdown partly restored the sensitivity to trastuzumab (Fig. 2A).

Cancer stem cells (CSCs) play a critical role in cancer initiation, progression, metastasis and drug resistance [39]. To investigate whether Cul7 mediated trastuzumab resistance is due to changes in the cancer stem cell population, we first assessed spheroid formation which is one of the characteristics of CSCs. Cul7 knockdown significantly inhibited spheroid formation capacities in SKBR3-TR-shCul7 cells and BT474-TR-shCul7 cells compared to corresponding TR-shCon cells (Fig. 2B). The expression of stem cell markers such as Nanog and Oct4 was also significantly decreased in SKBR3-TR-shCul7 and BT474-TR-shCul7 cells compared to corresponding TR-shCon cells (Fig. 2C). These results demonstrated that the increase in Cullin7 expression further activated CSCs, leading to resistance to trastuzumab treatment.

We also investigated the relationship among Cul7 expression, tumor-initiating capacity and trastuzumab resistance *in vivo*. Tumor xenografts were established in female BALB/c nude mice using SKBR3-TR shCon and shCul7 cells, and BT474-TR shCon and shCul7 cells. We found that tumor volumes were significantly smaller for SKBR3-TR-shCul7 and BT474-TR-shCul7 cells after trastuzumab treatment compared to corresponding TR-shCon cells (Fig. 2D and E).

Taken together, the increase in the expression of Cul7 occurs in trastuzumab-resistant Her2-amplified breast cancer cells, and reduction of Cul7 expression partly restores the resistance to trastuzumab treatment.

### 2.2. Cullin7 mediated trastuzumab resistance through regulation of the ratio of Ser/Tyr phosphorylation of IRS-1 by degrading Ser phosphorylated IRS-1

Increased insulin-like growth factor-1 receptor (IGF-1R) signaling has recently been identified as a potential factor adversely influencing the response to trastuzumab. IRS-1, a well-known substrate of the IGF-1R, activates PI3K through direct binding of the SH2 domains of the p85 regulatory subunit when tyrosine is phosphorylated [40]. To determine whether IRS-1/PI3K signaling is activated in parental and TR cells, p85 was immunoprecipitated from cells cultured in the presence or absence of trastuzumab, and the antibody pulldowns were probed with an anti-phosphotyrosine IRS-1 antibody. In TR cells, p-Tyr IRS-1 markedly interacted with p85 (Fig. 3A). We next investigated the upstream activator of IRS-1 in cells. As shown in Fig. 3B, IGF-1R was highly phosphorylated in only the TR cells, irrespective of trastuzumab treatment. Cul7 can participate in the degradation of IRS-1 in a mTOR/S6K dependent manner, which induced Ser phosphorylation of IRS-1 [37]. Most studies support that hyper-Ser/Thr phosphorylation acts as negative feedback to downregulate IRS-1 function and can eventually attenuate PI3K/Akt signaling [28]. To determine whether Cul7 participate in the regulation of IGF-1R/IRS-1 signaling, we first assessed the

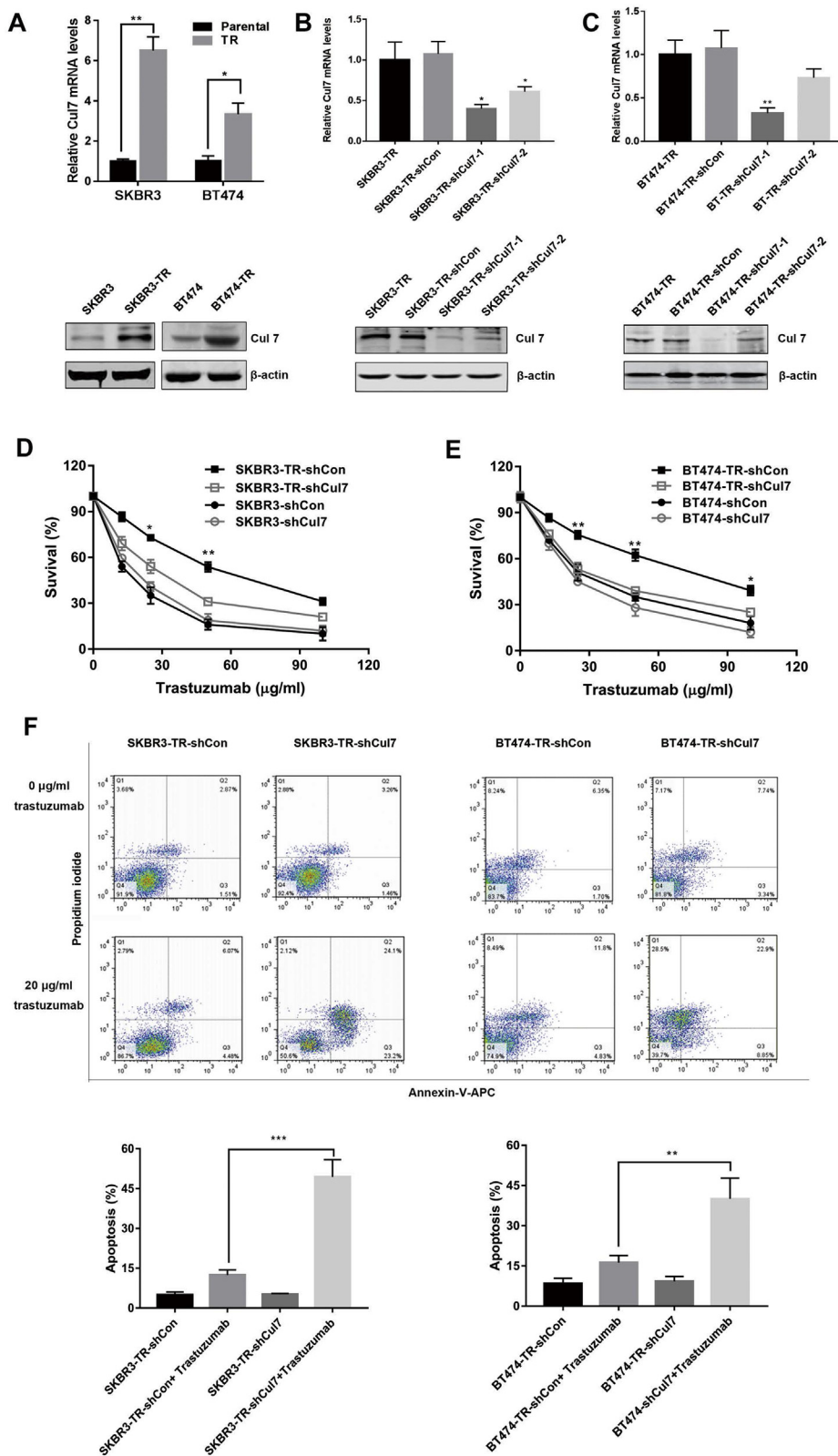


**Fig. 1.** Cullin7 level correlates with trastuzumab resistance of Her2 positive breast cancer cell line SKBR3 cells. Cul7 mRNA and protein levels were detected by real-time PCR and Western blotting (WB) in trastuzumab sensitive (SKBR3, BT474) and resistant (SKBR3-TR and BT474-TR) Her2 positive breast cancer cells (A). Cul7 was downregulated in SKBR3-TR (B) cells and BT474-TR cells (C). Cell viability was measured by MTS assay to demonstrate the effects of Cul7 expression on trastuzumab sensitivity in SKBR3-TR cells (D) and BT474-TR cells (E). Annexin V-APC/PI staining of cells treated for 72 h with 20 µg/mL trastuzumab in SKBR3-TR cells and BT474-TR cells (F). Data were expressed as means ± SD. All experiments were repeated in at least triplicate. \*, P < 0.05 versus corresponding shRNA control.

endogenous association of Cul7 and Tyr-phosphorylated IRS-1 (p-Tyr IRS-1) or Ser-phosphorylated IRS-1 (p-Ser IRS-1) through immunoprecipitation with an anti-Cul7 monoclonal antibody after IGF-1 stimulation. Consistent with other studies, we found that Cul7 only interacted with p-Ser IRS-1, not p-Tyr IRS-1 (Fig. 3C). We then used MG132 to inhibit proteasome-mediated protein degradation and

assessed the accumulation of ubiquitylated IRS-1. In SKBR3-TR shCon cells, abundant ubiquitylated IRS-1 accumulated upon MG132 treatment. In contrast, relative less ubiquitylated IRS-1 was observed in SKBR3-TR shCul7 cells (Fig. 3D). In addition, we measured the decay rate of p-Ser IRS-1 and p-Tyr IRS-1 in the presence of the protein synthesis inhibitor, cycloheximide (CHX). Depletion of Cul7 markedly

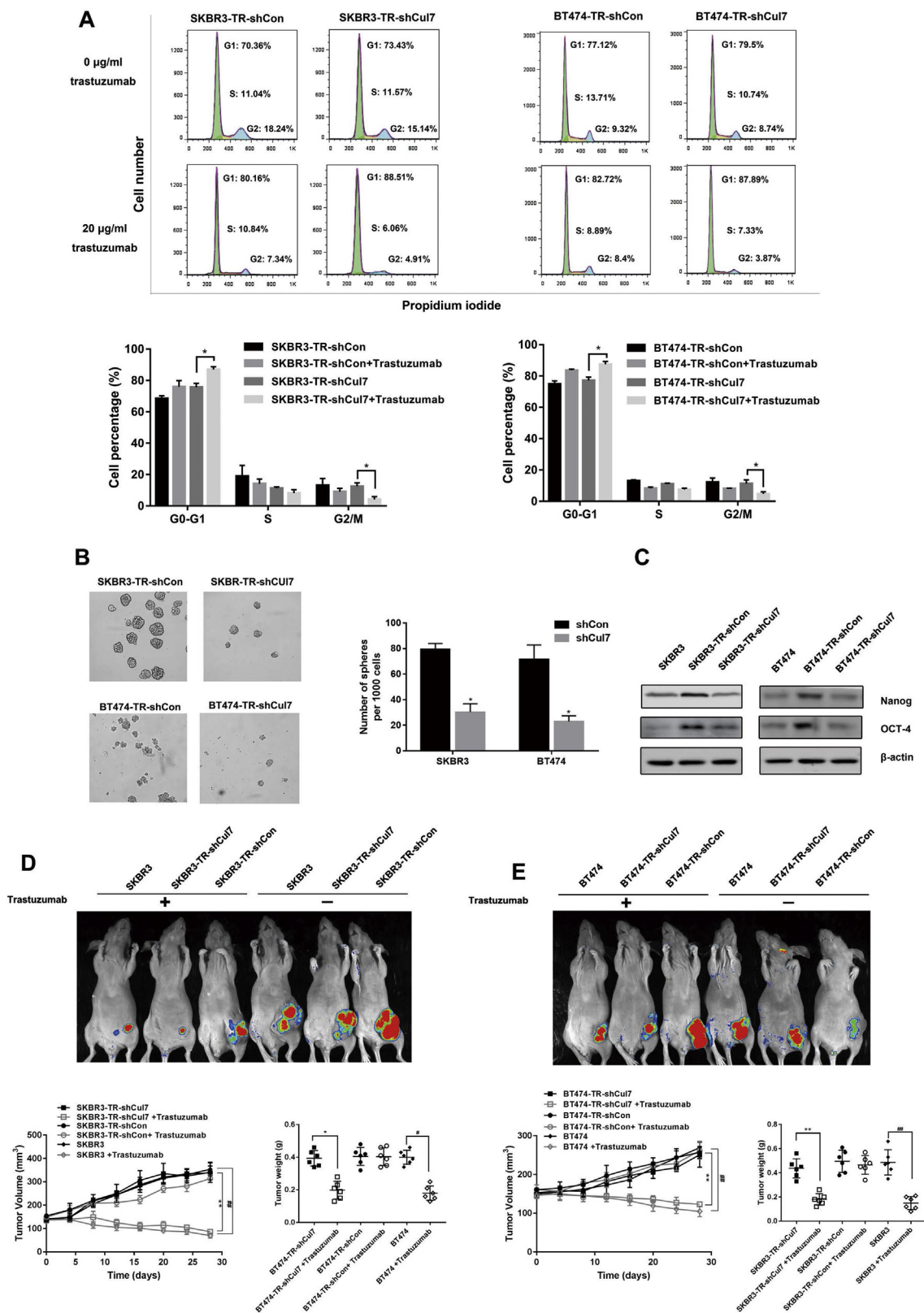


**Fig. 2.** Knockdown of Cullin7 induces cell cycle arrest and restores trastuzumab sensitivity in trastuzumab-resistant breast cancer cells. Cell cycle analysis of trastuzumab-resistant cells transfected with control (shCon.) or Cul7 shRNA treated for 48 h with 20 µg/mL trastuzumab (A). The spheroid formation of TR cells stably transfected with control (shCon.) or Cullin7 shRNA (B). CSC markers, such as Nanog and OCT4, were detected by Western blot analysis (C). Comparison of the growth curve of TR shCon and shCul7 cell-induced xenografts in mice treated with 30 mg/kg trastuzumab or saline water (n = 6). Average tumor volume is plotted against time (in days) (D-E). Data represent means ± S.D. \*\*, P < 0.01 versus corresponding TR shRNA control. ##, P < 0.01 versus corresponding parental cells.

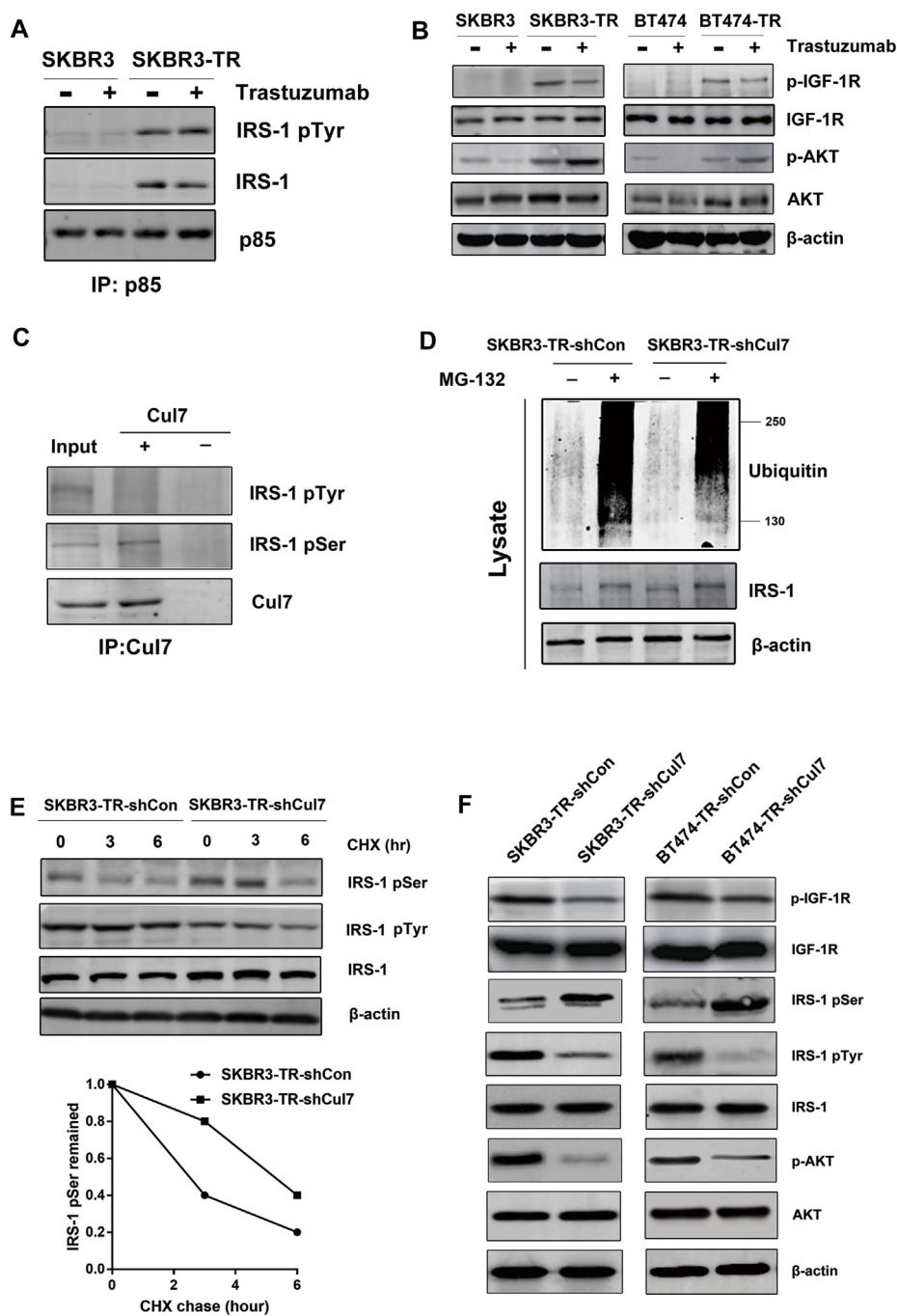


**Fig. 3.** Cullin7 degrades Ser-phosphor-IRS-1 in a ubiquitin dependent manner to enhance the IGF-1R/PI3K/Akt pathway. Parental and TR-cells were treated with or without 20 µg/ml trastuzumab for 6 h (B). Association between endogenous IRS-1 and CUL7. Extracts (1 mg of protein) from SKBR3-TR shCon cells were subjected to immunoprecipitation with anti-CUL7 (lane 2) or IgG (lane 3) antibodies, followed by Western blot analysis with p-Tyr and p-Ser IRS-1 (C). SKBR3-TR shCon and shCul7 cells were treated with or without 20 mM MG132 for 4 h prior to harvest. Ubiquitination levels and IRS-1 from total cell lysates were analyzed by Western blot analysis (D). SKBR3-TR shCon and shCul7 cells were treated with 10 mM cycloheximide (CHX) for the indicated times. Decreasing amounts of pre-existing IRS-1 protein levels were analyzed by Western blot analysis (E). Western blot analyses of the IGF-1R/PI3K/Akt pathway in TR shCon and shCul7-cells (F).

attenuated the decay rate of p-Ser IRS-1 in SKBR3-TR cells, which was consistent with previously published observations. However, the decay rate of p-Tyr IRS-1 was not changed by Cul7 (Fig. 3E). Next, we detected whether Cul7 regulated IGF-1R/IRS-1/AKT signaling in Her2-positive breast cancer cells. As shown in Fig. 3F, Cul7 knockdown led to accumulated p-Ser IRS-1, and it led to the reduction of phosphorylated IGF-1R, p-Tyr IRS-1 and phosphorylated Akt. These results indicated that Cul7 depletion attenuated the degradation of p-Ser IRS-1. Induction of p-Ser IRS-1 resulted in reduction of p-Tyr IRS-1, and then led to inhibition of the IGF-1R/IRS-1/PI3K/AKT signaling pathway to restore trastuzumab sensitivity.

**2.3. Cullin7 downregulated IGFBP-3 to activate the IGF-1R pathway inducing trastuzumab resistance**

To investigate how Cul7 affected p-IGF-1R in TR cells, we used RT-PCR to perform gene expression profiling experiments on the IGF-1R axis in the TR versus parental cells, TR-shCon cells and TR-shCul7 cells. We found that the mRNA expression of IGFBP-3, which is known to inhibit IGF-induced activation of IGF-1R, was downregulated in TR cells. However, IGFBP-3 mRNA was upregulated by Cul7 knockdown in TR cells (Fig. 4A and B). Similar results were obtained with the protein expression of IGFBP-3 (Fig. 4C and D). These results raise the possibility that Cul7 activates the IGF-1R pathway by inhibition of IGFBP-3 expression in the TR cells. Thus, we determined whether downregulation of IGFBP-3 in Cul7 knockdown TR cells would lead to reacquired resistance to trastuzumab. As shown in Fig. 4E and F, the TR-shCul7 cells

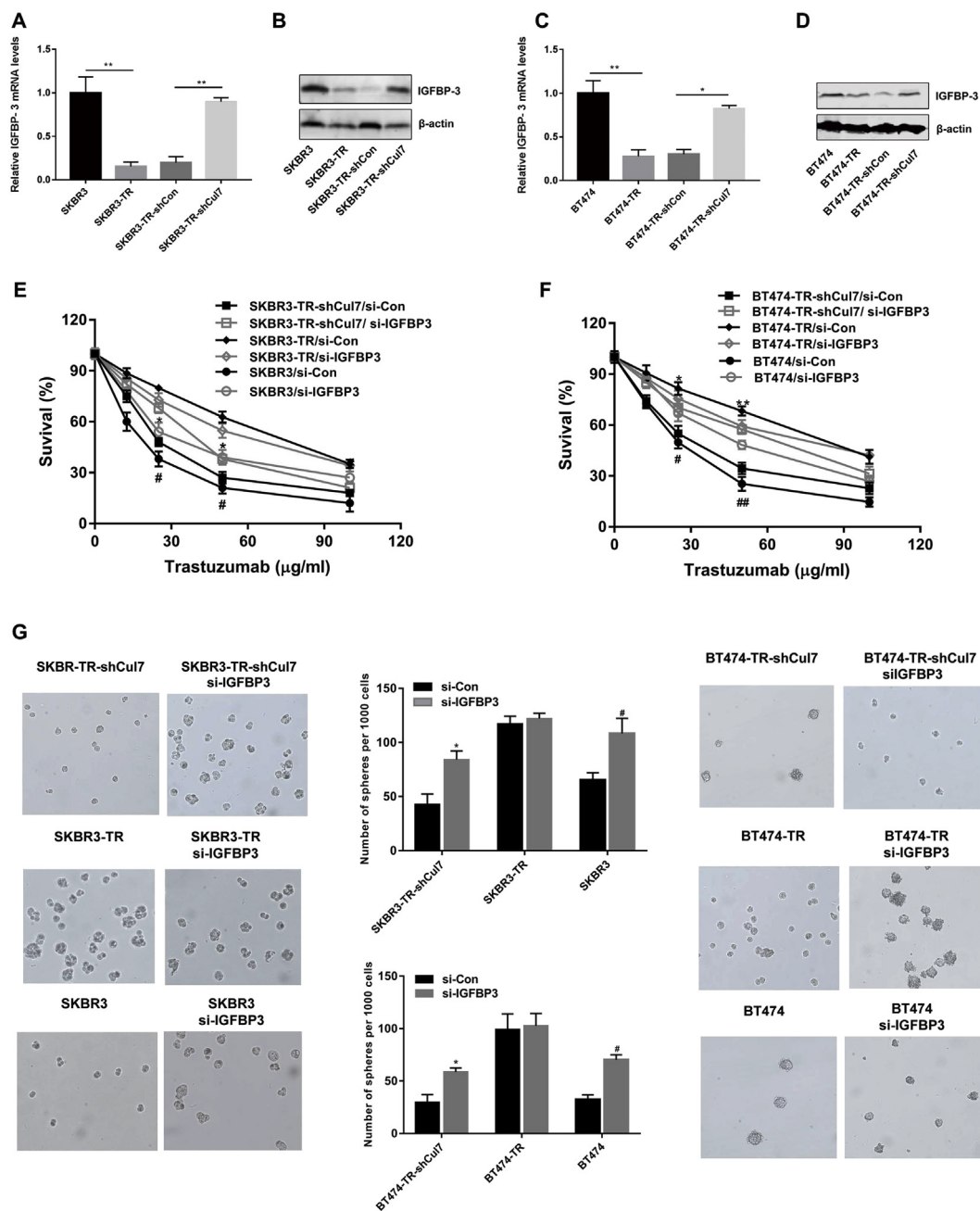


**Fig. 4. Cullin7 induces trastuzumab resistance partly dependent on IGFBP-3.** Real-time PCR analysis of IGFBP-3 mRNA expression in parental and TR-cells, TR shCon and shCul7 cells (A and B). Western blot analysis of IGFBP-3 protein expression in parental and TR-cells, TR shCon and shCul7 cells (C and D). Cells were exposed to a concentration range of trastuzumab (0–100 μg/ml) for 72 h, and cell viability was measured by MTS assay with growth in drug-free medium serving as control (E and F). The spheroid formation of TR-Cul7 cells stably transfected with control or IGFBP-3 shRNA (G). Data were represented as the means ± S.D. \*, P < 0.05; \*\*, P < 0.01 versus corresponding shRNA control or vehicle treatment. #, P < 0.05; ##, P < 0.01 versus corresponding parental cells control.

infected with the lentivirus containing IGFBP-3 shRNA became significantly resistant to trastuzumab. Cul7 knockdown TR cells with IGFBP-3 shRNA also had significantly enhanced spheroid formation capacities compared to corresponding shCon cells (Fig. 4G). Collectively, our studies suggest that Cul7 modulates trastuzumab sensitivity in Her2 positive breast cancer cells partly depended on IGFBP-3, and specific knockdown of IGFBP-3 significantly attenuates trastuzumab-mediated growth inhibition and apoptosis in Cul7 knockdown TR cells.

**2.4. Cullin7 is transcriptionally regulated by TCF7L2**

Several studies have implicated constitutively active Wnt/β-catenin signaling in breast cancer progression and CSC maintenance. Non-

phosphorylated β-catenin accumulates in the cytoplasm; when activated, it enters the nucleus and interacts with T-cell transcription factors to regulate transcription of various target genes that are involved in cellular proliferation, migration and CSC [41,42]. Some evidence demonstrates that IGFBP-3 is a novel and effective inhibitor of Wnt signaling. IGFBP-3 binds to the Wnt signalosome, interacting specifically with its component GSK-3β. As a consequence, the β-catenin destruction complex dissociates from LRP6 and is degraded by the proteasomal pathway in the cytoplasm [43]. To determine whether treatment with IGFBP-3 affected the cellular levels of β-catenin, SKBR3-TR cells and BT474-TR cells were exposed to IGFBP-3 and trastuzumab for 48 h, and the amount of β-catenin and phosphorylated Akt was verified from whole cell lysates by Western blotting. As shown in Fig. 5A and B,

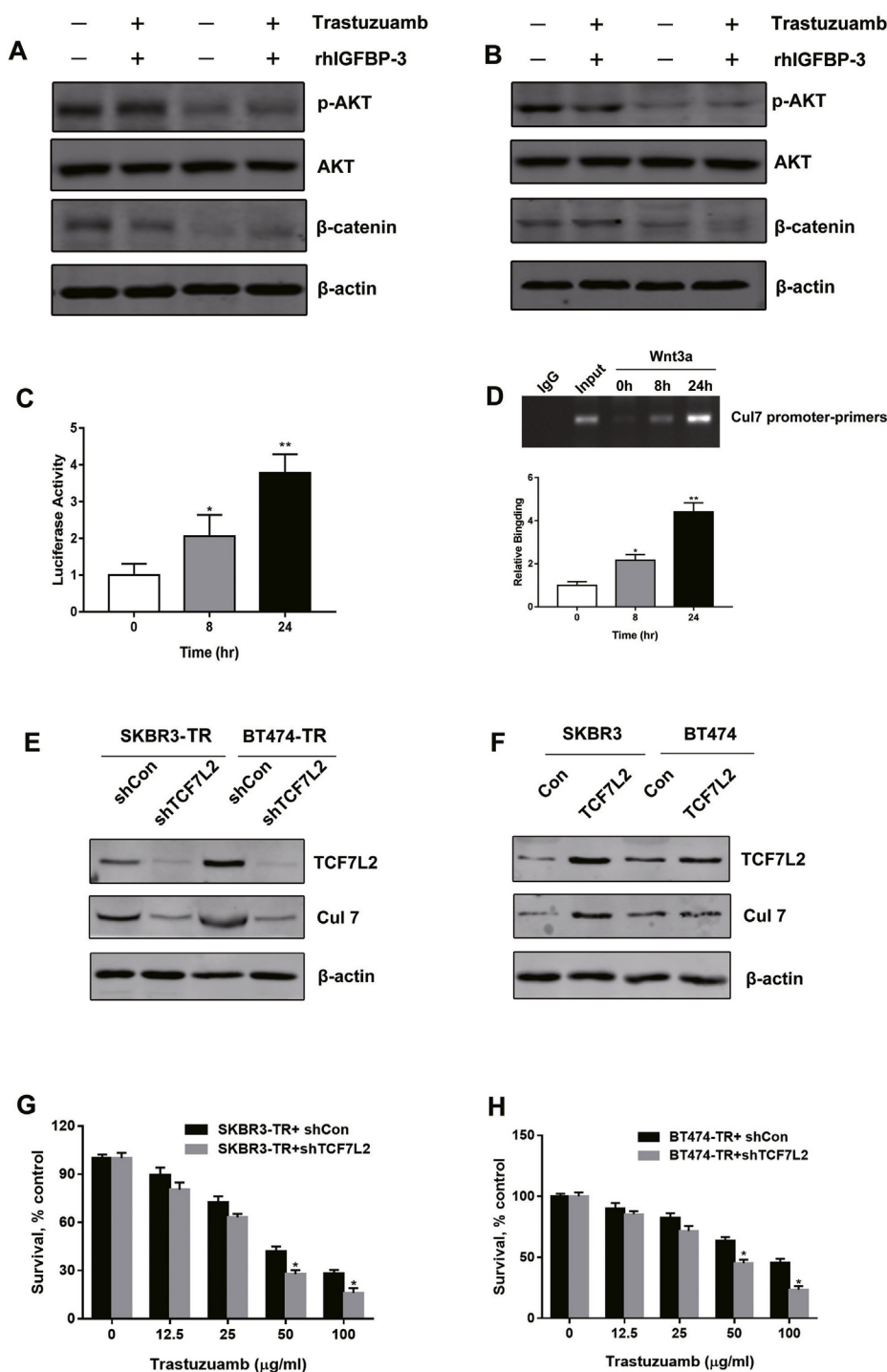


**Fig. 5. Transcription of Cul7 is regulated by TCF7L2.** SKBR-TR (A) and BT474-TR (B) cells were treated with IGFBP-3 (0.25  $\mu$ g/ml) and trastuzumab (20  $\mu$ g/ml) alone or in combination. Cell lysates were prepared and Western blot analysis was performed for p-AKT, total AKT and  $\beta$ -catenin. A luciferase reporter assay in HEK293 cells using the Cul7 promoter after Wnt3a stimulation (C). ChIP assay analyzed binding of TCF7L2 to a specific promoter region of Cul7 (D). Top panel shows agarose gel pictures of the PCR products. Western blot analysis of the protein expression of TCF7L2 and Cul7 in TR-cells with TCF7L2 shRNA (E) or overexpression of TCF7L2 (F). Cells were exposed to a concentration range of trastuzumab (0–100  $\mu$ g/ml) for 72 h, and cell viability was measured by MTS assay with growth in drug-free medium serving as control (G and H). Data were represented as the means  $\pm$  S.D. \*,  $P < 0.05$ ; \*\*,  $P < 0.01$  versus corresponding control or vehicle treatment.

treatment with IGFBP-3 drastically lowered the overall levels of  $\beta$ -catenin in both trastuzumab resistant cell lines. Interestingly, TCF7L2 is a T-cell transcription factor that is downstream of Wnt/ $\beta$ -catenin. The Cul7 promoter contains a number of putative binding sites for the TCF7L2. The effect of Wnt3a on Cul7 transcription was further assessed in HEK293 cells by Cul7 promoter-dependent luciferase activities assay (Fig. 5C). After 8 h of stimulation with Wnt3a, Cul7 promoter-dependent expression of luciferase was significant increased. The role of TCF7L2 in Cul7 transcription was examined by treating SKBR3-TR cells with Wnt3a for 8 h and 24 h and then performing chromatin immunoprecipitation (ChIP) using a TCF7L2 specific antibody. Binding of TCF7L2 to the Cul7 promoter was verified by RT-PCR using Cul7

promoter-specific primers. The ChIP analysis showed enhanced binding of TCF7L2 to the Cul7 promoter upon stimulation with Wnt3a compared to vehicle alone (Fig. 5D, upper and lower panels). TCF7L2 knockdown by RNA interference decreased Cul7 transcription in both SKBR3-TR and BT474-TR cells (Fig. 5E). In contrast, TCF7L2 overexpression in both breast cancer cell lines significantly increased Cul7 expression (Fig. 5F). As shown in Fig. 5G and H, the TR cells infected with lentivirus containing TCF7L2 shRNA became significantly sensitive to trastuzumab. Taken together, these findings establish the role of TCF7L2 as a transcription regulator of Cul7, and there are major implications for therapy in trastuzumab resistant patients.

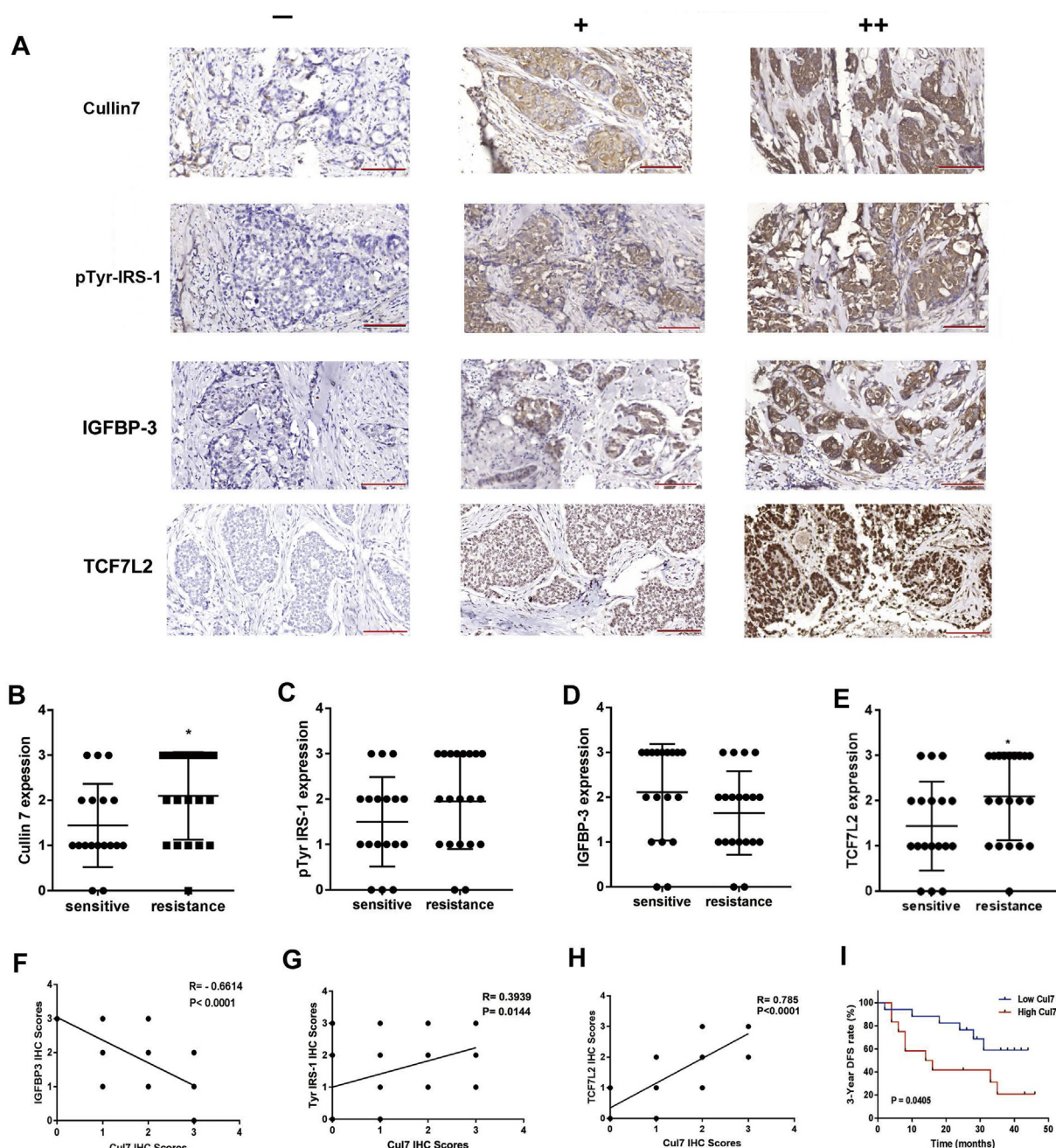


**Fig. 6. Cullin7 is positively correlated with trastuzumab resistance in breast cancer patients with Her2 amplification.** Representative micrographs of immunohistochemical staining of Cullin7, Tyr-phospho-IRS-1, and IGFBP-3 in trastuzumab-resistant and trastuzumab-sensitive breast cancers specimen (A). Scale bars, 50  $\mu$ m. The levels of Cul7 (B), Tyr-phospho-IRS-1 (C), IGFBP-3 (D) and TCF7L2 (E) in trastuzumab-resistant and trastuzumab-sensitive breast cancer specimens. \*,  $P < 0.05$  versus trastuzumab sensitive breast cancer. The correlation of Cul7 and IGFBP-3 (F), tyr-phospho-IRS-1 (G) or TCF7L2 (H) level in all trastuzumab-resistant and trastuzumab-sensitive breast cancer specimens. The period of disease-free survival of patients with high expression (+ + + + +; red columns) of Cullin7 and low expression (- / +, blue columns) of Cullin7 (I). (For interpretation of the references to colour in this figure legend, the reader is referred to the Web version of this article.)

**2.5. Cullin 7 is a predictive biomarker for response to trastuzumab in HER2-positive breast cancer patients**

To address the clinical implications of our findings, we examined the levels of Cul7, Tyr phosphorylation of IRS-1 and IGFBP-3 by IHC in a cohort of 38 Her2-positive primary invasive breast cancers obtained adjuvant trastuzumab treatment. The representative images of immunohistochemical staining of Cul7, Tyr phosphorylation of IRS-1, IGFBP-3 and TCF7L2 are presented in Fig. 6A. The expression of Cul7, Tyr phosphorylation of IRS-1 and TCF7L2 were negatively correlated

with trastuzumab sensitivity, while IGFBP-3 expression was positively correlated with trastuzumab sensitivity (Fig. 6B–E). Consistent with *in vitro* results, Cul7 expression was negatively correlated with IGFBP-3 expression, but it was positively correlated with Tyr phosphorylation of IRS-1 and TCF7L2 (Fig. 6F–H). Multivariate survival analysis showed that tumors with high Cul7 expression exhibited a statistically strong association with shorter DFS in patients receiving adjuvant trastuzumab-based therapy (Fig. 6I). This evidence further confirmed our findings that Cul7 could be used as a specific biomarker of trastuzumab response in HER2-positive breast cancer.

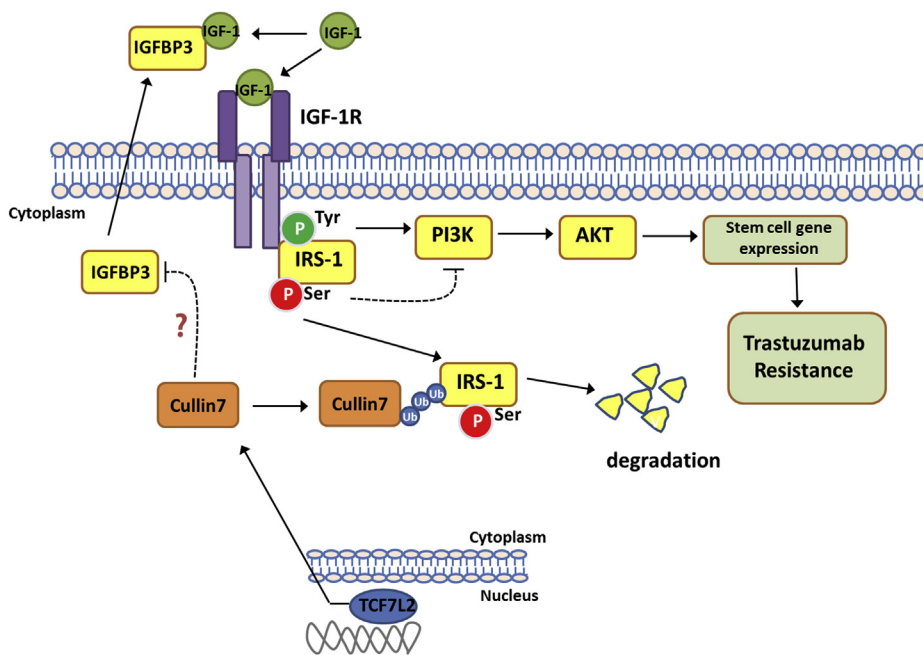


**Fig. 7.** Schematic model of the molecular mechanism linking Cullin7 and trastuzumab resistance in Her2 positive breast cancer via degrading IRS-1 and downregulating IGFBP-3 to activate the PI3K/AKT Pathway. Cullin7 degrades of Ser phosphorylation of IRS-1, activating the PI3K/AKT pathway, and inducing trastuzumab resistance in trastuzumab-resistant Her2 positive breast cancer cells. In addition, Cullin7 decreases IGFBP-3 expression, which leads to release of the Wnt signaling pathway inhibition and establishes positive feedback loop to an increase in Cullin7 expression, as mediated by TCF7L2 in trastuzumab-resistant Her2 positive breast cancer cells.

Based on the above results, a novel molecular mechanism linking Cullin7 and trastuzumab resistance in Her2 positive breast cancer via degrading IRS-1 and downregulating IGFBP-3 to activate the PI3K/AKT Pathway is established. Cullin7 degrades of Ser phosphorylation of IRS-1, activating the PI3K/AKT pathway, and inducing trastuzumab resistance in trastuzumab-resistant Her2 positive breast cancer cells. IGFBP-3 expression is decreased in trastuzumab-resistant Her2 positive breast cancer cells, which leads to release of the Wnt signaling pathway inhibition and an increase in Cullin7 expression, as mediated by TCF7L2 (Fig. 7).

### 3. Discussion

Cullin7 is a member of the cullin family of proteins that functions as scaffold proteins for E3 ubiquitin ligases. Like other members of the cullin family, such as Cul1, Cul3 and Cul4, Cul7 is a novel oncogene [35,36]. Overexpression of Cul7 mRNA and protein was significantly associated with poor prognosis and metastasis in patients with non-small cell lung carcinoma and hepatocellular carcinoma [44,45]. Forced expression of cullin7 enhanced cell migration, invasion and metastasis in human choriocarcinoma, breast cancer and liver cancer [45–47]. However, Cul7 mediated cancer cell resistance to drugs has not been reported. Our results found that Cul7 is highly expressed in trastuzumab-resistant breast cancer cells. The expression levels of Cul7 protein are statistically negatively correlated with DFS in patients receiving adjuvant trastuzumab-based therapy. Knockdown of Cul7 partly restores trastuzumab sensitivity, accompanied with activation of the IGF-1R/IRS-1/Akt pathway and induction of the cancer stem cell population. These results suggest that Cul7 mediated trastuzumab resistance in Her2 positive breast cancers through aberrant activation of PI3K/Akt signaling to induce cancer stem cell-like characteristics.

Resistance to HER2-targeted therapy might be associated with aberrant activation of the PI3K/Akt/mTOR pathway [48–50]. Some reports demonstrate that the activity of trastuzumab could be potentially impaired via induction of cell surface receptors such as IGF-1R [51]. Knockdown of IGF-1R significantly promote trastuzumab-mediated growth inhibition in trastuzumab resistant breast cancer cells. Knockdown of IGF-1R dramatically enhanced trastuzumab mediated inhibitory effects on P-erbB3 and P-Akt [52]. It is widely known that the PI3K/Akt pathway is downstream of IRS-1, and IRS-1 could be phosphorylated by IGF-1R [22]. Thus, the strength and duration of PI3K/Akt

pathway activity partly depends upon the level of IRS-1. Moreover, a lot of studies showed that IRS-1 contains several potential tyrosine phosphorylation sites and serine/threonine phosphorylation sites. Tyrosine phosphorylated of IRS1 can recruit the SH2 containing signal transducers including PI3K, positively regulates PI3K/Akt signaling; However, serine phosphorylation of IRS-1 at critical sites can block tyrosine phosphorylation and prevent IRS-1 binding to the IR, acting as a negative feedback to downregulate IRS-1 function [30]. The majority of serine/threonine phosphorylation of IRS-1 plays a regulatory role in the dissociation of IRS-1 from the receptor, blockage of specific tyrosine phosphorylation sites of IRS-1, cellular compartmentalization and degradation of IRS-1 [29]. Cul7 targets IRS-1 for ubiquitin-dependent degradation when mTORC1/S6K phosphorylates IRS-1 at serine residues, but Cul7 itself cannot degrade tyrosine phosphorylated IRS-1 [37]. Our results also demonstrated that Cul7 directly interacts with serine phosphorylated IRS-1 and degrades it. We found that compared with SKBR3-TR-shCul7 cells, SKBR3-TR cells that have high Cul7 expression and are trastuzumab-resistant had lower levels of serine phosphorylated IRS-1, but the level of tyrosine phosphorylated IRS-1 protein was relatively higher, sequentially leading to aberrant activation of the PI3K/Akt pathway. Clinical correlation analysis also demonstrated that Cul7 expression positively correlated with Tyr phosphorylation of IRS-1.

The IGF/IGF-binding protein (IGF/IGFBP) axis has been shown to influence the proliferation and survival of various tumors [53]. Several epidemiological studies have examined the relationship between the serum concentrations of IGF/IGFBPs and cancer incidence, emphasizing the idea that IGFs and IGFBPs may represent specific tumor markers [20]. IGFBP-3 is reported to be a growth suppressor by virtue of its effect on multiple pathways. In the IGF receptor dependent pathways, IGFBP-3 binds to IGF-1/2 and suppresses their growth signals. In our studies, the inhibition of IGFBP-3 expression occurred in trastuzumab-resistant Her2 positive breast cancer cells. IGFBP-3 was upregulated upon Cul7 knockdown in TR cells. The TR-shCul7 cells infected with the lentivirus containing IGFBP-3 shRNA became significantly resistant to trastuzumab. These data suggest that Cul7 induces trastuzumab resistance partly via releasing the inhibition effect of IGFBP-1 on IGF pathway, but how Cul7 regulates IGFBP-3 expression needed further investigation.

IGFBP-3 functions as a modulator of Wnt/ $\beta$ -catenin signaling [43]. IGFBP-3 interacts with certain molecular effectors of the Wnt complex

and induces  $\beta$ -catenin degradation by causing  $\beta$ -catenin dissociation from the Wnt receptor complex. Consistent with previous studies, our results also showed that treatment with IGFBP-3 drastically downregulated the overall levels of  $\beta$ -catenin in both trastuzumab resistant cell lines. Several studies have implicated constitutively active Wnt/ $\beta$ -catenin signaling in breast cancer progression and CSC maintenance. Nonphosphorylated  $\beta$ -catenin accumulates in the cytoplasm; when Wnt binds its ligand, this pathway is activated, and  $\beta$ -catenin enters the nucleus and interacts with T-cell transcription factors to control various target genes that are involved in cellular proliferation, migration and CSCs. Our results demonstrate that Wnt- $\beta$ -catenin activation triggers the binding of TCF7L2 to a TCF/LEF binding motif within the Cul7 promoter and enhances transcription of Cul7.

In conclusion, our data show that Cul7 reduces expression levels of Ser phosphorylation of IRS-1, which could relieve the blockade of Tyr phosphorylation of IRS-1, thereby enhancing PI3K/AKT signaling and inducing cancer stem cell-like characteristics and resistance to trastuzumab. Our study reveals that Cul7 also downregulates IGFBP-3 expression, which induces IGF pathway activation and makes a positive loop for trastuzumab resistance. As to the crosstalk of PI3K/AKT signaling, Wnt- $\beta$ -catenin activation triggers the binding of TCF7L2 to a TCF/LEF binding motif within the Cul7 promoter and enhanced transcription of Cul7, which also forms a positive feedback loop for the IGF/IRS-1/Akt pathway to enhance the resistance to trastuzumab. We propose that Cul7 may be used as a biomarker of trastuzumab responsiveness, leading to personalized cancer treatment protocols involving a Cul7 deletion in combination with trastuzumab.

## 4. Materials and methods

### 4.1. Reagents and antibodies

Trastuzumab was purchased from Roche (Switzerland). KU-0063794 and GANT61 were purchased from Selleckchem corporation (Texas, USA). MG132 and cycloheximide were purchased from Sigma-Aldrich (CA, USA). Recombinant human Wnt3a, IGF-1 and IGFBP-3 were purchased from R&D systems (Minnesota, USA). ShCul7, shIGFBP-3, shTCF7L2 and shCon lentivirus vectors were purchased from Shanghai Genechem Co., Ltd. (Shanghai, China). pEZX-Gluc plasmid for the Cul7 promoter was purchased from Guangzhou FulenGen Co., Ltd. (Guangzhou, China). Annexin V-APC/PI staining kit (KGA1030) was purchased from KeyGene bioTECH Ltd. (Nanjing, China).

For primary antibodies, human Cullin7 (#A300-233A) was purchased from Bethyl Laboratories; phospho-Akt (Ser473) (D9E) (#4060), Akt (#4691), PI3 kinase p85 (#4257),  $\beta$ -catenin (#8480), Ubiquitin antibody (#3933), IGF-1R (3027), p-IGF-1R(3021), Nanog (#8822), OCT-4 (#2890) and human  $\beta$ -actin (#4970) antibodies were purchased from Cell Signaling Technology; phospho-Tyr-612-IRS-1 (#44-816G), human IRS-1 (#PA5-29667), and phosphorylated IRS-1 (S636/639) (PA5-37613) were purchased from Invitrogen; and human IGFBP-3 (#ab76001) was purchased from Abcam. IRDye@680RD goat anti-rabbit IgG antibody (926-68071) and IRDye@800RD goat anti-rabbit IgG (926-32210) were purchased from Li-cor. All antibodies were diluted in Tris buffered saline with 0.1% Tween® 20 (TBST) containing 5% bovine serum albumin (BSA). All dilutions were prepared immediately before use.

### 4.2. Cell culture

SKBR3 parental and trastuzumab-resistant breast cancer cells, and BT474 parental and trastuzumab-resistant breast cancer cells were gifts from Dr. Liu Bolin of the University of Colorado Anschutz Medical Campus. All cells were cultured in DMEM supplemented with 10% fetal bovine serum. Trastuzumab-resistant breast cancer cells were maintained in standard culture media with trastuzumab (20  $\mu$ g/mL).

### 4.3. Lentivirus-mediated stable expression of shRNA

Lentiviral vectors with Cul7-shRNA, IGFBP-3-shRNA and TCF7L2-shRNA vectors were purchased from Shanghai Genechem Co., Ltd. Lentiviruses were produced by transfection of 293T cells with lentivirus vector and packaging mix using Lipofectamine 2000 (Invitrogen). After 48 h of transfection, viral supernatants were collected, filtered, and stored at  $-80^{\circ}\text{C}$  with polybrene (8 mg/ml, Sigma-Aldrich, St. Louis, MO, USA) until use. Cells stably expressing SKBR3-TR-shCon and SKBR3-TR-shCul7, and BT474-TR-shCon and SKBR3-TR-shCul7 were selected with puromycin (2 mg/ml).

### 4.4. Cell viability assay

Approximately 3000 cells/well were seeded in 96-well plates in standard culture conditions. Then, cells were treated with trastuzumab at indicated concentrations for indicated time. Cell survival was assessed by MTS assay. All experiments were performed at least in triplicate. Cell survival for all experiments is expressed as the percentage of viable cells compared with untreated cells.

### 4.5. Flow cytometer analysis

For apoptosis assays, the indicated cells were treated with trastuzumab at indicated concentrations and time points, and cells were collected and stained with Annexin V-APC and propidium iodide. Apoptotic cells were measured as cells staining positive for Annexin V-APC as assessed by fluorescence-activated cell sorting analysis (Becton Dickinson, Franklin Lakes, NJ).

For cell cycle analysis, the indicated cells were treated with trastuzumab at indicated concentrations for 24 h. Then cells were suspended and fixed overnight in 70% ethanol, and then stained with propidium iodide (50  $\mu$ g/mL) according to the manufacturer's instructions. DNA content was analyzed using a FACScan cytometer (Becton Dickinson, Franklin Lakes, NJ).

### 4.6. Mammosphere formation assay

Single cell suspensions (2000 cells/mL) were plated in ultralow attachment 24-well plates. DMEM/F-12, B27 supplement, 10 ng/ml EGF and FGF-2, 5 mg/ml insulin, and 0.5 mg/ml hydrocortisone were added. The number of mammospheres was quantified after 10 days. Image capture and morphological assessment were performed using a Leica microscope.

### 4.7. Real-time RT-PCR

For quantitative real time RT-PCR, 1 mg of total RNA was reverse-transcribed to cDNA using Superscript III following the manufacturer's protocol (Invitrogen). The reaction was performed using an ABI Prism 7900HT sequence detection system (Applied Biosystems) in accordance with the manufacturer's instructions. All qPCRs were performed in duplicate. For analysis, the  $\Delta\text{Ct}$  method was applied and fold-change was calculated ( $\Delta\Delta\text{Ct}$ ). All values were normalized to  $\beta$ -actin expression. The sequences of the primers are described in [Supplementary Table S1](#). Primers for RT-PCR were purchased from Invitrogen.

### 4.8. Western blotting

Cells were plated in plates at a proper density in culture medium and were treated as indicated. Cells were lysed in RIPA buffer containing protease inhibitor cocktail (Calbiochem). Western blotting for proteins was carried out as previously described [54].

#### 4.9. Immunoprecipitation

Cells were plated in 6-well plates and treated with IGF-1 for 12 h. The cell lysates were incubated with Cullin7 antibody overnight at 4 °C and then incubated with Protein A- or G- Sepharose (Sigma) for another 1 h at 4 °C. The beads were washed three times with RIPA buffer and boiled in loading sample buffer. The immunoprecipitated samples were separated by SDS-PAGE and analyzed by immunoblotting.

#### 4.10. Ubiquitination assay

Cells were seeded in 6-well plates at a density of  $1 \times 10^5$  cells/well. The cells were treated in the presence of MG132 (20 mM) for 6 h, and then the media was replaced with fresh culture media for 20 min at 37 °C and lysed in RIPA buffer. The lysates added to loading buffer were boiled for 5 min and subjected to immunoblot analysis.

#### 4.11. Luciferase assays

Luciferase reporter assays were carried out using the Luciferase Assay System (Promega). The Cul7 promoter luciferase reporter construct and pTK-Renilla construct were cotransfected into cells, and luciferase activity was measured by the Dual-Luciferase Reporter Assay System (Promega). The results are expressed as luciferase/renilla ratios and represent the Mean  $\pm$  s.d. of at least three experiments, each performed in triplicate.

#### 4.12. ChIP assay

ChIP was performed according to the manufacturer's instructions (Cell Signaling Technology, 9003S). Briefly, the chromatin/DNA protein complexes were prepared from cells treated with vehicle (PBS with 0.1% BSA) or Wnt3a (30 ng/ml) for 2 h. Chemical crosslinking of DNA-proteins was carried out using 1% formaldehyde for 10 min at room temperature. The crosslinking was quenched by addition of glycine (0.125 M) for 5 min at room temperature, and then cells were scraped into PBS containing 1 mM PMSF. The cell suspension was centrifuged and the pellet was mixed by inverting the tube every 3 min in buffer A + DTT + PIC + PMSF, followed by incubation on ice for 10 min. The pellet (nuclei) was dissolved in 1.0 ml buffer B + DTT + 5 ml of micrococcal nuclease and incubated for 20 min at 37 °C with frequent mixing to digest DNA to a length of approximately 150–900 bp. To immunoprecipitate the chromatin, the lysate was incubated with appropriate ChIP-grade TCF-4 (TCF7L2) antibody (sc-8631, Santa Cruz Biotechnology, Inc.) overnight at 4 °C with rotation, followed by ChIP-grade protein G magnetic beads and incubation for 2 h at 4 °C with rotation. The magnetic beads were washed using buffers supplied with the kit. The eluted DNA was purified and analyzed by PCR to determine the binding of TCF7L2 to the Cul7 promoter. PCR primers were designed using the criteria described in the kit. The region of the human Cul7 promoter from –490 to –760 bp was taken to design the primers and found to bear the putative TCF7L2 binding site (consensus sequence: AGATCAAAGG) identified by online transcription factor binding prediction software (Jaspar 2018; <http://jaspar.genereg.net/>). The following primers were used: human Cul7-forward (F) 5'-TCCCA AAGTGCTGGGATTAC-3', and human Cul7-reverse (R) 5'-GTTTGTAT GATCAACGTTG-3'. Real-time PCR amplification was performed using iQ SYBR Green Supermix (Bio-Rad) and an ABI Prism 7900HT sequence detection system (Applied Biosystems).

#### 4.13. In vivo sensitivity test

All studies were approved by the Committee on the Ethics of Animal Experiments of Guangzhou Medical University and complied fully with the recommendations in the Guide for the Care and Use of Laboratory Animals of the Guangzhou Medical University. Cells ( $1 \times 10^6$  cells/

mouse) were injected subcutaneously (s.c.) into the flank of BALB/c node female mice. Body weight and tumor volume were measured every 3 days. Once tumor volumes reached 400–500 mm<sup>3</sup>, seven to eight mice were randomized to each treatment or control group. Mice were primed with an initial loading dose of trastuzumab at 6.0 mg/kg by i.p. injection and then received a maintenance dose of 3 mg/kg twice weekly. At the termination of the study, all mice were sacrificed, and tumors were collected for sequential analysis.

#### 4.14. Immunohistochemistry

Specimens were obtained from 38 female breast cancer patients with HER2 gene amplification before neoadjuvant trastuzumab therapy in the breast tumor surgical department, affiliated Cancer Hospital and Institute of Guangzhou Medical University, from July 2013 to March 2016. Patients are defined as trastuzumab sensitivity if clinical responses to trastuzumab therapy are classified as complete response (CR, complete disappearance of the lesion), partial response (PR, 30% or more decrease in the lesion from pre-treatment size), or stable disease (SD, reduction in size of the tumor less than 30%) by imaging assessment. Patients are defined as trastuzumab resistance if clinical responses to trastuzumab therapy are classified as progressive disease (PD, at least a 20% increase in size of the lesion). The paraffin-embedded tissue sections were for studies of histology immunohistochemistry. All samples were collected with informed consent according to the internal review and ethics boards of the hospital (2016-180).

Cul7, Tyr-phosphorylated IRS-1 and IGF1R-3 expression were examined by immunohistochemistry on paraffin-embedded tissue sections according to previous research [55]. Whole slide digital images of each breast cancer sample were captured with the Aperio Scanscope AT2 slide scanner (collagen). The percentage of positive staining tumor cells was calculated per field of view, with at least 20 view fields per section evaluated at  $\times 200$  magnification.

#### 4.15. Statistical analysis

Numerical data are presented as the means  $\pm$  SD from at least 3 independent experiments performed in triplicate. Significance was assessed using two tailed Student's t-tests, with a P-value  $< 0.05$  considered to be significant. Statistical analysis was performed by one-way analysis of variance, and comparisons among groups were performed by independent sample t-test or Bonferroni's multiple comparison tests. To measure the association between variables, Spearman correlations were used.

#### Conflicts of interest

The authors declare that they have no competing interests.

#### Acknowledgements

This study was supported by the Natural Science Foundation of Guangdong Province (2017A030313551, 2018A030310174), Program of Bureau of Education of Guangzhou Municipality (1201630281), Program of Bureau of Health of Guangzhou Municipality (20161A011082, 20171A010315), the National Natural Science Foundation of China (81772803, 81402187), and the Scientific and Technological Planning Project of Guangzhou City (201805010002). The funders had no role in study design, data collection and analysis, decision to publish, or preparation of the manuscript. We thank Dr. Zhijie Zhang for his generosity in sharing reagents and flow cytometry analysis.

#### Appendix A. Supplementary data

Supplementary data to this article can be found online at <https://>

doi.org/10.1016/j.canlet.2019.08.008.

## References

- [1] Michael D. Brooks, Monika L. Burness, Max S. Wicha, Therapeutic implications of cellular heterogeneity and plasticity in breast cancer, *Cell Stem Cell* 17 (2015) 260–271.
- [2] P. Eroles, A. Bosch, J. Alejandro Pérez-Fidalgo, A. Lluch, Molecular biology in breast cancer: intrinsic subtypes and signaling pathways, *Cancer Treat Rev.* 38 (2012) 698–707.
- [3] S. Koren, M. Bentires-Alj, Breast tumor heterogeneity: source of fitness, hurdle for therapy, *Mol. Cell* 60 (2015) 537–546.
- [4] F. Montemurro, S. Di Cosimo, G. Arpino, Human epidermal growth factor receptor 2 (HER2)-positive and hormone receptor-positive breast cancer: new insights into molecular interactions and clinical implications, *Ann. Oncol. Off. J. Eur. Soc. Med. Oncol.* 24 (2013) 2715–2724.
- [5] A. Prat, et al., Clinical implications of the intrinsic molecular subtypes of breast cancer, *Breast* 24 (Suppl 2) (2015) S26–S35.
- [6] C.A. Santa-Maria, L. Nye, M.B. Mutonga, S. Jain, W.J. Gradishar, Management of metastatic HER2-positive breast cancer: where are we and where do we go from here? *Oncology* 30 (2016) 148–155.
- [7] S. Ahmed, A. Sami, J. Xiang, HER2-directed therapy: current treatment options for HER2-overexpressing breast cancer, *Breast Canc.* 22 (2015) 101–116.
- [8] C.L. Arteaga, et al., Treatment of HER2-positive breast cancer: current status and future perspectives, *Nat. Rev. Clin. Oncol.* 9 (2011) 16–32.
- [9] M.C. Figueroa-Magalhaes, D. Jelovac, R. Connolly, A.C. Wolff, Treatment of HER2-positive breast cancer, *Breast* 23 (2014) 128–136.
- [10] G.L. Fiszman, M.A. Jasnis, Molecular mechanisms of trastuzumab resistance in HER2 overexpressing breast cancer, *Int. J. Breast Canc.* 2011 (2011) 352182.
- [11] P. Gonzalez-Alonso, et al., Recent insights into the development of preclinical trastuzumab-resistant HER2+ breast cancer models, *Curr. Med. Chem.* 25 (2018) 1976–1998.
- [12] A. Madrid-Paredes, M. Canadas-Garre, A. Sanchez-Pozo, M.A. Calleja-Hernandez, De novo resistance biomarkers to anti-HER2 therapies in HER2-positive breast cancer, *Pharmacogenomics* 16 (2015) 1411–1426.
- [13] E. Olson, D. Mullins, When standard therapy fails in breast cancer: current and future options for HER2-positive disease, *J. Clin. Trials* 3 (2013) 1000129.
- [14] F. Puglisi, A.M. Minisini, C. De Angelis, G. Arpino, Overcoming treatment resistance in HER2-positive breast cancer: potential strategies, *Drugs* 72 (2012) 1175–1193.
- [15] M.A. Alaoui-Jamali, G.B. Morand, S.D. da Silva, ErbB polymorphisms: insights and implications for response to targeted cancer therapeutics, *Front. Genet.* 6 (2015) 17.
- [16] A. Dittich, H. Gautrey, D. Browell, A. Tyson-Capper, The HER2 signaling network in breast cancer-like a spider in its web, *J. Mammary Gland Biol. Neoplasia* 19 (2014) 253–270.
- [17] R. Roskoski Jr., The ErbB/HER family of protein-tyrosine kinases and cancer, *Pharmacol. Res.* 79 (2014) 34–74.
- [18] D.F. Stern, ERBB3/HER3 and ERBB2/HER2 duet in mammary development and breast cancer, *J. Mammary Gland Biol. Neoplasia* 13 (2008) 215–223.
- [19] Y.S. Chun, M. Huang, L. Rink, M. Von Mehren, Expression levels of insulin-like growth factors and receptors in hepatocellular carcinoma: a retrospective study, *World J. Surg. Oncol.* 12 (2014) 231.
- [20] B.Y. Hernandez, et al., Differences in IGF-axis protein expression and survival among multiethnic breast cancer patients, *Cancer Med.* 4 (2015) 354–362.
- [21] Y. Higashi, S. Sukhanov, A. Anwar, S.Y. Shai, P. Delafontaine, Aging, atherosclerosis, and IGF-1. *The journals of gerontology, J. Gerontol. Ser. A Biol. Med. Sci.* 67 (2012) 626–639.
- [22] S.R. Keller, L. Lamphere, B.E. Lavan, M.R. Kuhne, G.E. Lienhard, Insulin and IGF-1 signaling through the insulin receptor substrate 1, *Mol. Reprod. Dev.* 35 (1993) 346–351 discussion 351–342.
- [23] L.M. Shaw, The insulin receptor substrate (IRS) proteins: at the intersection of metabolism and cancer, *Cell Cycle* 10 (2011) 1750–1756.
- [24] E. Van Obberghen, Signalling through the insulin receptor and the insulin-like growth factor-1 receptor, *Diabetologia* 37 (Suppl 2) (1994) S125–S134.
- [25] R. Baserga, The insulin receptor substrate-1: a biomarker for cancer? *Exp. Cell Res.* 315 (2009) 727–732.
- [26] B.T.-Y. Chan, A.V. Lee, Insulin receptor substrates (IRSs) and breast tumorigenesis, *J. Mammary Gland Biol. Neoplasia* 13 (2008) 415–422.
- [27] H.A. Porter, A. Perry, C. Kingsley, N.L. Tran, A.D. Keegan, IRS1 is highly expressed in localized breast tumors and regulates the sensitivity of breast cancer cells to chemotherapy, while IRS2 is highly expressed in invasive breast tumors, *Cancer Lett.* 338 (2013) 239–248.
- [28] K.D. Capps, M.F. White, Regulation of insulin sensitivity by serine/threonine phosphorylation of insulin receptor substrate proteins IRS1 and IRS2, *Diabetologia* 55 (2012) 2565–2582.
- [29] B. Draznin, Molecular mechanisms of insulin resistance: serine phosphorylation of insulin receptor substrate-1 and increased expression of p85alpha: the two sides of a coin, *Diabetes* 55 (2006) 2392–2397.
- [30] P. Gual, Y. Le Marchand-Brustel, J.-F. Tanti, Positive and negative regulation of insulin signaling through IRS-1 phosphorylation, *Biochimie* 87 (2005) 99–109.
- [31] J. Mercado-Matos, J.L. Clark, A.J. Piper, J. Janusis, L.M. Shaw, Differential involvement of the microtubule cytoskeleton in insulin receptor substrate 1 (IRS-1) and IRS-2 signaling to AKT determines the response to microtubule disruption in breast carcinoma cells, *J. Biol. Chem.* 292 (2017) 7806–7816.
- [32] D.C. Dias, G. Dolios, R. Wang, Z.Q. Pan, CUL7: a DOC domain-containing cullin selectively binds Skp1.Fbx29 to form an SCF-like complex, *Proc. Natl. Acad. Sci. U.S.A.* 99 (2002) 16601–16606.
- [33] D. Hanson, et al., Mutations in CUL7, OBSL1 and CCDC8 in 3-M syndrome lead to disordered growth factor signalling, *J. Mol. Endocrinol.* 49 (2012) 267–275.
- [34] J. Yan, et al., The 3M complex maintains microtubule and genome integrity, *Mol. Cell* 54 (2014) 791–804.
- [35] S.S. Kim, et al., CUL7 is a novel antiapoptotic oncogene, *Cancer Res.* 67 (2007) 9616–9622.
- [36] V. Paradis, et al., Cullin7: a new gene involved in liver carcinogenesis related to metabolic syndrome, *Gut* 62 (2013) 911–919.
- [37] X. Xu, et al., The CUL7 E3 ubiquitin ligase targets insulin receptor substrate 1 for ubiquitin-dependent degradation, *Mol. Cell* 30 (2008) 403–414.
- [38] T. Vu, F.X. Claret, Trastuzumab: updated mechanisms of action and resistance in breast cancer, *Front. Oncol.* 2 (2012) 62.
- [39] H. Korkaya, M.S. Wicha, HER2 and breast cancer stem cells: more than meets the eye, *Cancer Res.* 73 (2013) 3489–3493.
- [40] S. Guo, Insulin signaling, resistance, and the metabolic syndrome: insights from mouse models into disease mechanisms, *J. Endocrinol.* 220 (2014) T1–t23.
- [41] W.H. Matsui, Cancer stem cell signaling pathways, *Medicine* 95 (2016) S8–S19.
- [42] R. Nusse, H. Clevers, Wnt/beta-Catenin signaling, disease, and emerging therapeutic modalities, *Cell* 169 (2017) 985–999.
- [43] A. Naspi, et al., IGFBP-3 inhibits Wnt signaling in metastatic melanoma cells, *Mol. Carcinog.* 56 (2017) 681–693.
- [44] J. An, et al., Overexpression of Rabl3 and Cullin7 is associated with pathogenesis and poor prognosis in hepatocellular carcinoma, *Hum. Pathol.* 67 (2017) 146–151.
- [45] D. Zhang, G. Yang, X. Li, C. Xu, H. Ge, Inhibition of liver carcinoma cell invasion and metastasis by knockdown of Cullin7 in vitro and in vivo, *Oncol. Res.* 23 (2016) 171–181.
- [46] H. Guo, F. Wu, Y. Wang, C. Yan, W. Su, Overexpressed ubiquitin ligase Cullin7 in breast cancer promotes cell proliferation and invasion via down-regulating p53, *Biochem. Biophys. Res. Commun.* 450 (2014) 1370–1376.
- [47] J. Fu, et al., Ubiquitin ligase cullin 7 induces epithelial-mesenchymal transition in human choriocarcinoma cells, *J. Biol. Chem.* 285 (2010) 10870–10879.
- [48] I. Mayer, Role of mTOR inhibition in preventing resistance and restoring sensitivity to hormone-targeted and HER2-targeted therapies in breast cancer, *Clin. Adv. Hematol. Oncol. : HO (Hum. Organ.)* 11 (2013) 217–224.
- [49] J.A. McCubrey, et al., Ras/Raf/MEK/ERK and PI3K/PEN/Akt/mTOR cascade inhibitors: how mutations can result in therapy resistance and how to overcome resistance, *Oncotarget* 3 (2012) 1068–1111.
- [50] J.A. McCubrey, et al., Therapeutic resistance resulting from mutations in Raf/MEK/ERK and PI3K/PEN/Akt/mTOR signaling pathways, *J. Cell. Physiol.* 226 (2011) 2762–2781.
- [51] A. Camirand, Y. Lu, M. Pollak, Co-targeting HER2/ErbB2 and insulin-like growth factor-1 receptors causes synergistic inhibition of growth in HER2-overexpressing breast cancer cells, *Med. Sci. Monit. : Int. Med. J. Exp. Clin. Res.* 8 (2002) BR521–526.
- [52] X. Huang, et al., Heterotrimerization of the growth factor receptors erbB2, erbB3, and insulin-like growth factor-i receptor in breast cancer cells resistant to herceptin, *Cancer Res.* 70 (2010) 1204–1214.
- [53] C.E. Tognon, P.H. Sorensen, Targeting the insulin-like growth factor 1 receptor (IGF1R) signaling pathway for cancer therapy, *Expert Opin. Ther. Targets* 16 (2012) 33–48.
- [54] N. Qiu, et al., Disruption of Kif3a in osteoblasts results in defective bone formation and osteopenia, *J. Cell Sci.* 125 (2012) 1945–1957.
- [55] A.S. McCampbell, et al., Loss of inhibitory insulin receptor substrate-1 phosphorylation is an early event in mammalian target of rapamycin-dependent endometrial hyperplasia and carcinoma, *Cancer Prev. Res.* 3 (2010) 290–300.